Inhibition of dentine caries using fluoride solution with silver nanoparticles: An in vitro study

Iris Xiaoxue Yin [1], Ollie Yiru Yu [1], Irene Shuping Zhao [2], May Lei Mei [3] *, Quan Li Li [4], Jinyao Tang [5], Edward Chin Man Lo [1], Chun Hung Chu [1]*

[1] Faculty of Dentistry, the University of Hong Kong, Hong Kong, China

[2] School of Stomatology, Shenzhen University Health Science Center, Shenzhen, China

[3] Department of Oral Rehabilitation, Faculty of Dentistry, University of Otago, New Zealand

[4] College of Stomatology, Anhui Medical University, Hefei, China

[5] Department of Chemistry, the University of Hong Kong, Hong Kong, China

Key words: *Silver nanoparticles, fluoride, caries, dentine, remineralisation*

Correspondence to : * Dr. ML Mei
Department of Oral Rehabilitation
Faculty of Dentistry
University of Otago
Dunedin, New Zealand
E-mail: may.mei@otago.ac.nz

* Prof. CH Chu
Faculty of Dentistry
The University of Hong Kong
34 Hospital Road, Hong Kong SAR, China
E-mail: chchu@hku.hk

Abstract

Objectives*: To investigate the remineralising and staining effects of sodium fluoride (NaF) with silver nanoparticles (AgNPs) on artificial dentine caries.*

Methods: *Human dentine blocks with artificial caries were divided into four groups. Group 1 received 5% NaF (22,600 ppm fluoride) with 4,000 ppm AgNPs; group 2 received 4,000 ppm AgNPs; group 3 received 5% NaF, group 4 received deionised water (negative control). All groups underwent three biochemical cycles. Each cycle included Streptococcus mutans biofilm challenge and remineralisation process. The lesion depth, mineral-organic content, surface morphology and crystal characteristics of dentine blocks were evaluated using micro-computed tomography, Fourier transform infrared spectroscopy, scanning electron microscopy (SEM) and X-ray diffraction. Colour change of dentine blocks was assessed using spectrophotometry.*

Results: *The mean lesion depths of groups 1 to 4 were 151.13 ± 29.13µm, 172.38 ± 23.44µm, 190.41 ± 32.81µm and 221.24 ± 27.91µm, respectively. The hydrogen phosphate-to-amide I ratios of groups 1 to 4 were 5.98 ± 0.36, 3.86 ± 0.56, 4.00 ± 0.67 and 2.53 ± 0.40, respectively. There was no significant interaction effect between AgNPs and NaF. SEM showed less exposure of dentine collagen fibres in group 1 when compared to other groups. X-ray diffraction revealed presence of silver chloride and metallic silver in group 1 and 2. There was no significant difference in colour change among the four groups ($p = 0.74$).*

Conclusions: *NaF solution with AgNPs can remineralise dentine caries without staining.*

Clinical Significance: *Sodium fluoride solutions that include silver nanoparticles have potential uses in the management of caries.*

Introduction

Contemporary caries management awareness has shifted from the traditional surgical approach to a medical model that includes the use of fluoride therapy [1]. Sodium fluoride (NaF) varnish is one of the most common topical fluoride products for the prevention of caries. It has been shown to substantially inhibit caries in both permanent and primary teeth [2]. Apart from prevention, NaF has also been used to arrest caries. However, its arresting rate on dentine caries is unsatisfactory [3, 4].

Overpopulation of acid-producing bacteria in the oral cavity is one of the main pathological factors of the cariogenic process. One of the limitations of NaF application is that its antibacterial effects may be negligible [5]. Therefore, a clinical protocol of adjunctive application of NaF with silver nitrate was introduced [6]. A recent clinical trial found that a semi-annual application of 25% silver nitrate followed by 5% NaF was no worse than an application of 38% silver diamine fluoride in arresting dentine caries (caries arresting rate: 64.1% and 62.4%, respectively) among preschool children [7]. Clinical studies have shown that 38% silver diamine fluoride arrests coronal caries in preschool children and root caries in elderly subjects [8]. The adjunctive application of silver nitrate and NaF has shown to be an equivalent alternative to silver diamine fluoride in both *in vitro* and *in vivo* studies [7, 9]. However, a side effect of using silver compounds is that the carious lesions are stained black. Even after being informed of this result, patients may not be pleased with the treatment's aesthetic outcomes.

One possible way to address the displeasing aesthetic effects of silver ion solutions is to use a fluoride solution that includes silver nanoparticles (AgNPs). Unlike silver ion solutions, which tend to form intense, black-coloured silver oxide layers, the intrinsic optoelectronic properties of AgNPs result in significantly less tooth discolouration [10]. We developed biocompatible AgNPs using epigallocatechin gallate in a previous study [11]. These AgNPs have been shown to inhibit cariogenic species growth and do not stain teeth. However, whether these AgNPs can be applied adjunctively with NaF to arrest caries has not been studied. Hence, we aim to investigate the remineralising effect of the application of the NaF with AgNPs on dentine caries. The null-hypothesis is that the adjunctive application of AgNPs and NaF can remineralise artificial dentine caries without significant staining on the carious lesion.

Materials and Method

Synthesis of silver nanoparticles

The synthesis of AgNPs in an aqueous solution was carried out via chemical reduction of silver nitrate with epigallocatechin gallate as reducing agent and chitosan as dispersant. First, 0.5 mL silver nitrate (50 mM) was mixed with 20 mL chitosan (10 mg/mL, pH=5), which was previously dissolved in 0.2% (v/v) acetic acid. Then, under continuous magnetic stirring, 1 mL epigallocatechin gallate (50 mM) was added dropwise to the mixed solution. The reaction mixture was stirred 10 minutes to ensure the formation and even growth of nanoparticles, and the unreacted starting reagents were removed by washing three times with a centrifuge [11].

Preparing blocks with artificial dentine caries

This study received approval from the Institutional Review Board (IRB UW14-529). The study's protocol is shown in Figure 1. Thirty molars were collected from patients who required the extraction of such teeth after gaining the patients' consent. Dentine slices with a thickness of 2 mm were prepared from the extracted molars. The slices' surfaces were polished using micro-fine 4000-grit sanding paper. Polished slices with flaws or other defects were excluded. Each slice was cut into four blocks for further treatment. Half of the blocks' surface was coated with acid-resistant nail varnish to acted as an internal control. The blocks were sterilised by autoclaving at 121°C [12].

Streptococcus mutans was employed to create artificial caries. The microorganisms were cultured anaerobically on blood agar plates at 37°C for 2 days. An isolated colony was selected from each agar plate and re-suspended in brain heart infusion (BHI) with 5% glucose to McFarland 2 (6×10^8 cells/mL). Subsequently, blocks were soaked in the wells of 24-well plate containing 1 ml of bacteria culture in BHI with 5% glucose. The plates were placed in an anaerobic chamber (FORMA ANAEROBIC CHAMBER; THERMO FISHER SCIENTIFIC Inc., MA, USA) at 37°C for 3 days which provides an anaerobic atmosphere for incubation of *Streptococcus mutans* biofilm. The biofilm created carious lesion on the surface of exposed dentine blocks which is approximately 70 μm in depth [13]. The blocks were then sterilised by autoclaving at 121°C.

Experimental treatment

The blocks were then randomised distributed to four groups. In Group 1, the blocks received a topical application of AgNPs (4,000 ppm silver) solution followed by 5% NaF solution (22,600 ppm fluoride). In Group 2, the blocks received a topical application of AgNPs solution (4,000 ppm silver). In Group 3, the blocks received a topical application of 5% NaF solution (22,600 ppm fluoride). In Group 4, the blocks were treated with deionised water (negative control). Microbrushes (Micro applicator-regular; Premium Plus International Ltd., Hong Kong, China) were used to apply all solutions to the blocks' surfaces. The solution was left on surface of blocks for 10 minutes before they were experience further treatment. The treatments all groups received were one-off.

Biochemical cycling

The treated blocks were cycled using a biochemical model. The model contains a biofilm challenge and chemical remineralisation (Figure 1). For the biofilm challenge, *S. mutans* bacterial suspensions were prepared in a BHI broth (pH = 7.5) to a cell density of McFarland 2 (6×10^8 cells/mL). Afterwards, a 300-µl aliquot of bacterial suspension was inoculated on each block. Each block was then put into 1 ml BHI medium with 5% glucose solution. After a 12-hour biofilm challenge, the blocks were rinsed with deionised water and immersed in an ultrasonic bath for 10 minutes to remove the biofilm. Subsequently, the blocks were immersed in an artificial saliva solution (pH 7.0) containing 20 mM 4-(2-hydroxyethyl)-1-piperazineethanesulfonic acid, 1.5 mM calcium chloride, 0.9 mM potassium dihydrogen phosphate and 150 mM potassium chloride [14]. The blocks were sterilised by autoclaving at 121°C before each cycle. The cycles were performed for 3 days before evaluation.

Lesion depth and mineral loss

Micro-computed tomography (micro-CT) (SkyScan 1172; SkyScan, Antwerp, Belgium) was used to scan the blocks to measure lesion depth and mineral loss. The X-ray source was operated at a voltage of 100 kV and a current of 80 kA. The image pixel size was set to 6 µm. A 0.5-mm aluminium filter was used to cut off the softest X-rays. The scanning results were reconstructed using NRecon reconstruction software (SkyScan, Antwerp, Belgium). CTAn data-analysis software (CTAn, Skyscan NV, Kontich, Belgium) was used to view and process the reconstructed three-dimensional images. Using each block's reconstructed image, cross-sectional images were located. Fifteen cross-sectional images were randomly selected to evaluate the lesion depth. The groups' mean lesion depths and mineral losses were measured

using CTAn data-analysis software with internal control as a reference line [14]. The reference line was a virtual line which was formed by extending from non-demineralised part of block surface to the surface of carious lesion [15]. Eight blocks per group were assessed.

Chemical structure

Potential changes in the chemical structure on the demineralised dentine surfaces were analysed using Fourier transform infrared spectroscopy (FTIR) with the infrared radiation wavelengths ranging from 550 to 2000 cm^{-1}. The ratio (HPO_4^{2-} : amide I) of the areas of absorbance from the phosphate HPO_4^{2-} peak, which was between 900 and 1200 cm^{-1}, to the amide I peak, which was between 1585 and 1720 cm^{-1}, was indicated the extent of the dentine's demineralisation. Eight blocks per group were assessed [13].

Surface morphology

Each block was fixed in 2.5% glutaraldehyde at 4°C for 4 hours. They were washed in distilled water, then dehydrated in a series of ethanol solutions (70% for 10 minutes, 95% for 10 minutes and 100% for 20 minutes). The blocks were then critical-point dried in a desiccator and sputter-coated with carbon. Scanning electron microscopy (SEM) (Hitachi S-4800 FEG Scanning Electron Microscope; Hitachi Ltd., Tokyo, Japan) was used to examine the blocks' surface morphology. Three blocks per group were assessed [16].

Crystal characteristics

X-ray diffraction (XRD) data were collected from each group using an X-ray diffractometer equipped with a scintillation counter. These data were collected with a range of 20–60° 2q, a step size of 0.05° and a scan speed of 30 seconds/step. The diffraction data were re-collected to reduce systematic errors after preliminary data collection. The International Centre for Diffraction Data (ICDD, PDF-2 Release 2004) database was used to check the phase purity and indexing of the chemical phase. The Bruker DIFFRAC plus EVA software was used to analyse the diffraction patterns. Three blocks per group were assessed [17].

Colour test

Colour tests were performed before the blocks received the topical application of the four treatments, as well as after 3 cycles. A VITA Easyshade Advance Portable Dental Spectrophotometer (VITA Zahnfabrik GmbH, Bad Säckingen, Germany) was used to examine the colours. The Commission International del'Eclairage L* a* b* colour system was applied

to measure the colour of each block. The L* axis represented lightness and ranged from black (0) to white (100), the a* axis represented red (+a*) to green (-a*), and the b* axis represented yellow (+b*) to blue (-b*). The equation $\triangle E = [(\triangle L^*)^2 + (\triangle a^*)^2 + (\triangle b^*)^2]^{1/2}$ was used to obtain the total colour change ($\triangle E$) after cycling. Eight blocks per group were assessed.

Statistical analysis

The characteristics of crystal by XRD and surface morphology by SEM were observed and not subjected to statistical analyses. The Shapiro-Wilk normality test was used to assess whether the data distribution was normal. A two-way ANOVA was used to compare the lesion depth and the HPO_4^{2-} : amide I ratio data. A one-way ANOVA with Bonferroni multiple comparison tests was used to compare $\triangle E$ values among the four treatment groups. Analyses were performed using SPSS Statistics – V20.0 computer software (IBM Corporation, Armonk, NY, USA). The level of statistical significance for all tests was 0.05.

Results

The typical micro-CT images of the blocks in the four treatment groups are shown in Figure 2. The mean values ± standard deviation of lesion depth and mineral loss are shown in Table 1. The blocks treated with AgNPs + NaF exhibited the lowest lesion depth (151.13 µm ± 29.13 µm) and mineral loss (0.65 g/µm^3 ± 0.05 g/µm^3) among all the groups. According to the results of the two-way ANOVA (Table 2), whether the blocks received treatment with AgNPs and treatment with NaF had a significant effect on lesion depth and mineral loss ($p < 0.001$). There was no significant interaction effect between AgNPs and NaF treatment for lesion depth ($p = 0.40$) and mineral loss ($p = 0.88$).

The mean values ± standard deviation of the HPO_4^{2-} : amide I absorbance ratio in Group 1 through 4 were 5.98 ± 0.36, 3.86 ± 0.56, 4.00 ± 0.67 and 2.53 ± 0.40, respectively. Figure 3 shows the representative FTIR spectra on the surface of dentine blocks in the four treatment groups. A two-way ANOVA (Table 3) showed that AgNPs and NaF functioned as two variables had significant effects on the HPO_4^{2-} : amide I ratio ($p < 0.001$). There was no significant interaction effect between these two variables ($p = 0.13$).

It was observed that dentine collagen fibres were barely exposed on the relatively smooth surfaces of the blocks in in Group 1 (AgNPs + NaF) (Figure 4). Compared to Group 1,

block surfaces and even inter-tubular areas in Groups 2 (AgNPs) and 3 (NaF) exposed more dentine collagen. Dentine collagens were sparsely distributed with an increased inter-fibrillar distance in blocks of Group 4, which had relatively rough surfaces.

Typical XRD spectra from the four groups are presented in Figure 5. Diffraction peaks were detected at $2\theta = 31.8°$, $2\theta = 32.9°$ and $2\theta = 39.8°$, which corresponded to the peaks for hydroxyapatite (211, 300 and 310). The lower intensity of peaks 211, 300 and 310 in the water group spectra indicated the loss of dentine due to the dissolution of the hydroxyapatite crystal structure. In addition, prominent diffraction peaks were detected at 32.2° and 46.3° in the spectra of groups with AgNPs (Groups 1 and 2), which corresponded to silver chloride (200 and 220). The peak at $2\theta = 38.18°$ and $2\theta = 44.27°$ represented the detection of silver (111 and 200) in Group 1 and 2, implying the presence of metallic silver [17].

The values of the chromatic coordinates L* a* b* are shown in Table 4. The intragroup analysis of lightness (L*) values presented no significant decline in all groups after 3 cycles ($p > 0.05$). All four groups displayed an obvious collapse in the value of a* ($p < 0.05$). In particular, Group 2 (AgNPs) dropped from 20.37 ± 2.88 to 15.56 ± 1.85 ($p < 0.001$). The b* values of the four groups did not significantly change ($p > 0.05$). The $\triangle E$ of Group 1 through 4 were 6.92 ± 3.11, 7.09 ± 1.84, 6.30 ± 2.79 and 6.77 ± 2.44, respectively. There was no significant difference ($p = 0.74$) among all four groups.

Discussion

Biocompatible AgNPs were successfully synthesised using epigallocatechin gallate and chitosan in our previous study [11]. We demonstrated that these AgNPs had low toxicity against human gingival fibroblasts and stem cells from human exfoliated deciduous teeth and inhibited *S. mutans* biofilm growth. In this study, the adjunctive application of AgNPs and NaF was used to remineralise artificial dentine caries. The remineralising effect of AgNPs and NaF on dentine caries was measured with lesion depth, mineral loss, mineral-organic content, surface morphology and crystal characteristics using micro-CT, FTIR, SEM and XRD. The results showed that treatment with AgNPs and NaF can remineralise artificial dentine caries without significant staining on the carious lesion.

To simulate the cariogenic challenges in the mouth, various demineralisation-remineralisation models have been used for cariology research. In particular, the pH-cycling model is commonly used. It is intended to mimic the *in vivo* periodic alternation of pH, which occurs in the mouth when sugars are metabolised [18]. However, the pH-cycling model does not include biological factors. Therefore, it cannot mimic the breakdown of dentine's organic matrix by bacteria-derived enzymes, and the antimicrobial properties of the treatment can be underestimated. Therefore, we replaced the demineralised solution with the *S. mutans* mono-species biofilm challenge used in the current study. We measured the acidity (pH) of the culture medium before we performed the pH cycling, but we did not monitor the pH. This is a limitation of this study. This combination of chemical and microbiological models not only provides periodic pH alternation, but also supplies a microbiological environment for bacterial impact. Moreover, the advantages of using mono-species biofilm include the fact that that the bacteria cells' growth and accumulation and the biofilm's physiological properties can be accurately investigated [18]. Compared with multi-species biofilm, mono-species biofilm with consistent structure and composition is not involved in the uncontrolled fluctuations of specific oral environment. Nevertheless, the interactions of different bacteria, such as competition, cross-feeding or colony succession cannot be considered [19].

AgNPs adjunctively applied with NaF on carious dentine surfaces do not influence the remineralising effect of NaF or the anti-biofilm effect of AgNPs. Dentine treated with NaF or AgNPs showed shallower lesion depth and less mineral loss than dentine in groups without NaF or AgNPs ($p < 0.01$). The high fluoride concentrations in this study can promote the remineralisation of dentine lesions. Fluoride deposited on the dentine surface can produce CaF_2 which is a temporary fluoride reservoir. At low pH, F ions are released from unstable CaF_2 and subsequently replace the hydroxyl ion in hydroxyapatite, converting to fluorapatite [20]. The solubility of fluorapatite is lower than that of hydroxyapatite in an acidic environments, which means the hard tissue of the teeth has stronger acid resistance and is less likely to demineralise. However, because the difference between fluorapatite and hydroxyapatite is below the detection threshold of XRD [21], we could not distinguish between them in the current study. The micro-CT results indicated that artificial dentine caries in groups treated with NaF underwent more effective remineralisation than those in groups treated without NaF. In addition, caries in groups treated with AgNPs also underwent more effective remineralisation. This effect could relate to the superior and long-acting antimicrobial effect of AgNPs against *S. mutans*, which we demonstrated in our previous study [11]. AgNPs can denature the plasma

membrane after penetrating the bacterial membrane and interrupt DNA replication. AgNPs can also release Ag to intracellularly produce reactive oxygen species which disturb protein synthesis and cause cell lysis. Due to their nano-scale size and large amount of released Ag, AgNPs possess stronger antibacterial effect even than those of silver compounds against both planktonic and colonised bacteria. AgNPs can kill bacteria at low concentrations and decrease the kinetics and viability of the biofilm. Therefore, AgNPs can inhibit lactic acid, which accounts for 70% of the organic acid produced by oral biofilm and is considered a key factor that causes the demineralisation of teeth [22]. Hence, AgNPs can weaken the intensity of demineralisation through acid inhibition. There was no significant interaction effect between AgNPs and NaF, which indicates the blocks treated NaF with AgNPs had enhanced acid resistance and reduced demineralisation.

Dentine's mineral matrix is mainly composed of biological apatite, which is a group of phosphate minerals. The organic matrix of dentine is 90% type I collagen. Amide I is the main infrared absorption band of the peptide group in collagen and is related to the helical structure of collagen. In the FTIR spectra (Figure 3), the phosphate band represented the mineral matrix, the amide I band represented the organic matrix and the HPO_4^{2-} : amide ratio I related to the extent of demineralisation of dentine [23]. This study's results indicated that the HPO_4^{2-} : amide I ratio was higher on dentine surfaces treated with AgNPs and NaF than those without AgNPs and NaF, which suggests that AgNPs and NaF can decrease dentine demineralisation. AgNPs inhibit the dissolution of hydroxyapatite and the exposure of collagen by decreasing the production of acids from oral biofilm, as mentioned above. In addition, silver can prevent collagen degradation on demineralised dentine surfaces through the suppression of the catalytic functions of bacterial collagenase. As a scaffold, the preserved collagen benefits the deposition of mineral crystals and inhibits the diffusion of calcium and phosphate for further demineralisation [24]. The FTIR results also indicated there was no significant interaction between NaF and AgNPs. The application of NaF does not affect the inhibition effect of AgNPs on the dentine demineralisation.

Silver chloride was detected on the dentine surfaces of blocks in groups treated with AgNPs + NaF and AgNPs. Silver phosphate and silver oxide are supposed to be the products of the reaction between Ag ions and hydroxyapatite, which were actually not detected in the present study. The solubilities of silver phosphate and silver oxide are higher than that of silver chloride, so they can react with chlorides to yield silver chloride. This is consistent with our

previous studies [16, 25]. Silver compounds, particularly silver diamine fluoride, have been widely used in clinical settings for caries management. Although 38% silver diamine fluoride is regarded as sufficient to arrest caries, the undesirable side effect of this method is black staining on arrested caries. Silver chloride, as the principal precipitation found on tooth surfaces, may be the main reason for the black staining caused by silver diamine fluoride [5]. This aesthetic problem limits the applications of silver compounds. AgNPs demonstrated a priming colour effect when compared to silver compound due to their promising optoelectronic properties [11]. This study's results also included little colour change in dentine treated with AgNPs and NaF even after the biofilm challenge and remineralisation solution cycles (Table 4), which indicates that this application is unlikely to cause staining in clinical situations. Therefore, sodium fluoride solutions with silver nanoparticles have potential uses to manage caries.

Conclusions

This laboratory study demonstrated that a NaF solution that included AgNPs can remineralise artificial dentine caries without significant staining.

Declarations of interest

The authors declare that they have no conflict of interest.

References

[1] C.H. Chu, M.L. Mei, E.C. Lo, Use of fluorides in dental caries management, Gen Dent 58(1) (2010) 37-43; quiz 44-5, 79-80.

[2] V.C. Marinho, H.V. Worthington, T. Walsh, J.E. Clarkson, Fluoride varnishes for preventing dental caries in children and adolescents, Cochrane Database Syst Rev (7) (2013) CD002279.

[3] C.H. Chu, E.C. Lo, H.C. Lin, Effectiveness of silver diamine fluoride and sodium fluoride varnish in arresting dentin caries in Chinese pre-school children, J Dent Res 81(11) (2002) 767-70.

[4] D. Duangthip, C.H. Chu, E.C. Lo, A randomized clinical trial on arresting dentine caries in preschool children by topical fluorides--18 month results, J Dent 44 (2016) 57-63.

[5] M.L. Mei, E.C.M. Lo, C.H. Chu, Arresting Dentine Caries with Silver Diamine Fluoride: What's Behind It?, J Dent Res 97(7) (2018) 751-758.

[6] S.S. Gao, I.S. Zhao, S. Duffin, D. Duangthip, E.C.M. Lo, C.H. Chu, Revitalising Silver Nitrate for Caries Management, International journal of environmental research and public health 15(1) (2018).

[7] S.S. Gao, D. Duangthip, M.C.M. Wong, E.C. Lo, C.H. Chu, Randomized Trial of Silver Nitrate with Sodium Fluoride for Caries Arrest, JDR Clinical & Translational Research (2019).

[8] H.P. Tan, E.C. Lo, J.E. Dyson, Y. Luo, E.F. Corbet, A randomized trial on root caries prevention in elders, J Dent Res 89(10) (2010) 1086-90.

[9] I.S. Zhao, M.L. Mei, Q.L. Li, E.C.M. Lo, C.H. Chu, Arresting simulated dentine caries with adjunctive application of silver nitrate solution and sodium fluoride varnish: an in vitro study, Int Dent J 67(4) (2017) 206-214.

[10] A. Besinis, T. De Peralta, R.D. Handy, Inhibition of biofilm formation and antibacterial properties of a silver nano-coating on human dentine, Nanotoxicology 8(7) (2014) 745-54.

[11] I.X. Yin, O.Y. Yu, I.S. Zhao, M.L. Mei, Q.L. Li, J. Tang, C.H. Chu, Developing biocompatible silver nanoparticles using epigallocatechin gallate for dental use, Arch Oral Biol 102 (2019) 106-112.

[12] K. Preston, S. Higham, Pw, The efficacy of techniques for the disinfection of artificial sub-surface dentinal caries lesions and their effect on demineralization and remineralization in vitro, Journal of Dentistry 35(6) (2007) 490-495.

[13] M.L. Mei, Q.L. Li, C.H. Chu, E.C.M. Lo, L.P. Samaranayake, Antibacterial effects of silver diamine fluoride on multi-species cariogenic biofilm on caries, Ann Clin Microb Anti 12 (2013).
[14] O.Y. Yu, M.L. Mei, I.S. Zhao, E.C. Lo, C.H. Chu, Effects of Fluoride on Two Chemical Models of Enamel Demineralization, Materials (Basel) 10(11) (2017).
[15] Y.P. Qi, N. Li, L.N. Niu, C.M. Primus, J.Q. Ling, D.H. Pashley, F.R. Tay, Remineralization of artificial dentinal caries lesions by biomimetically modified mineral trioxide aggregate, Acta Biomaterialia 8(2) (2012) 836-842.
[16] O.Y. Yu, I.S. Zhao, M.L. Mei, E.C.M. Lo, C.H. Chu, Caries-arresting effects of silver diamine fluoride and sodium fluoride on dentine caries lesions, J Dent 78 (2018) 65-71.
[17] M.L. Mei, L. Ito, Y. Cao, Q.L. Li, E.C. Lo, C.H. Chu, Inhibitory effect of silver diamine fluoride on dentine demineralisation and collagen degradation, J Dent 41(9) (2013) 809-17.
[18] O.Y. Yu, I.S. Zhao, M.L. Mei, E.C.-M. Lo, C.-H. Chu, A review of the common models used in mechanistic studies on demineralization-remineralization for cariology research, Dentistry journal 5(2) (2017) 20.
[19] O.Y. Yu, I.S. Zhao, M.L. Mei, E.C.-M. Lo, C.-H. Chu, Dental Biofilm and Laboratory Microbial Culture Models for Cariology Research, Dentistry journal 5(2) (2017).
[20] X. Li, J. Wang, A. Joiner, J. Chang, The remineralisation of enamel: a review of the literature, Journal of Dentistry 42(S1) (2014) S12-S20.
[21] M.L. Mei, L. Ito, Y. Cao, E.C.M. Lo, Q.L. Li, C.H. Chu, An ex vivo study of arrested primary teeth caries with silver diamine fluoride therapy, Journal of Dentistry 42(4) (2014) 395-402.
[22] H. Chen, B. Zhang, M.D. Weir, N. Homayounfar, G.G. Fay, F. Martinho, L. Lei, Y. Bai, T. Hu, H.H.K. Xu, S. mutans gene-modification and antibacterial resin composite as dual strategy to suppress biofilm acid production and inhibit caries, J Dent (2020) 103278.
[23] H.K. Yip, J. Guo, W.H.S. Wong, Protection Offered by Root-surface Restorative Materials against Biofilm Challenge, Journal of Dental Research 86(5) (2007) 431-435.
[24] I.S. Zhao, S.S. Gao, N. Hiraishi, M.F. Burrow, D. Duangthip, M.L. Mei, E.C.M. Lo, C.H. Chu, Mechanisms of silver diamine fluoride on arresting caries: a literature review, International Dental Journal, 2018, pp. 67-76.
[25] O.Y. Yu, I.S. Zhao, M.L. Mei, E.C.M. Lo, C.H. Chu, Caries-arresting effects of silver diamine fluoride and sodium fluoride on dentine caries lesions, Journal of Dentistry 78 (2018) 65-71.

Figure 1. Flow chart of the experimental design

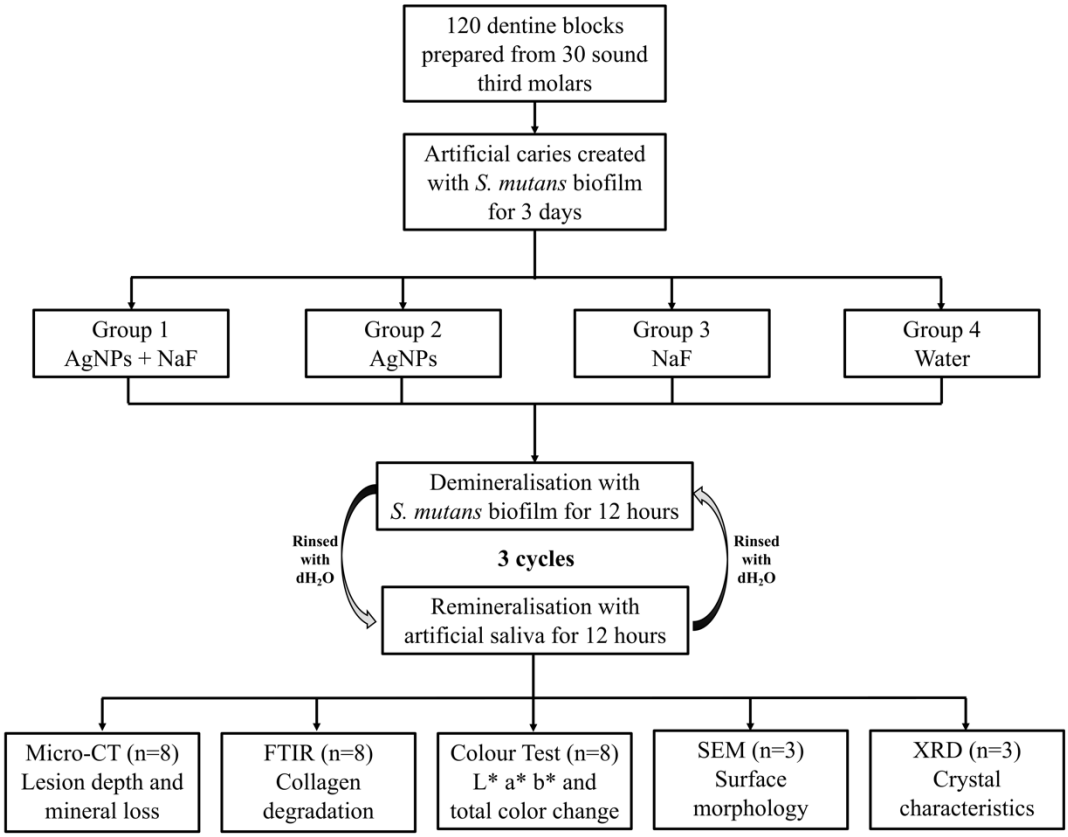

Figure 2. Representative micro-CT images (left column) and reconstructed three-dimensional images (right column) of artificial dentine carious lesions in the treatment groups.

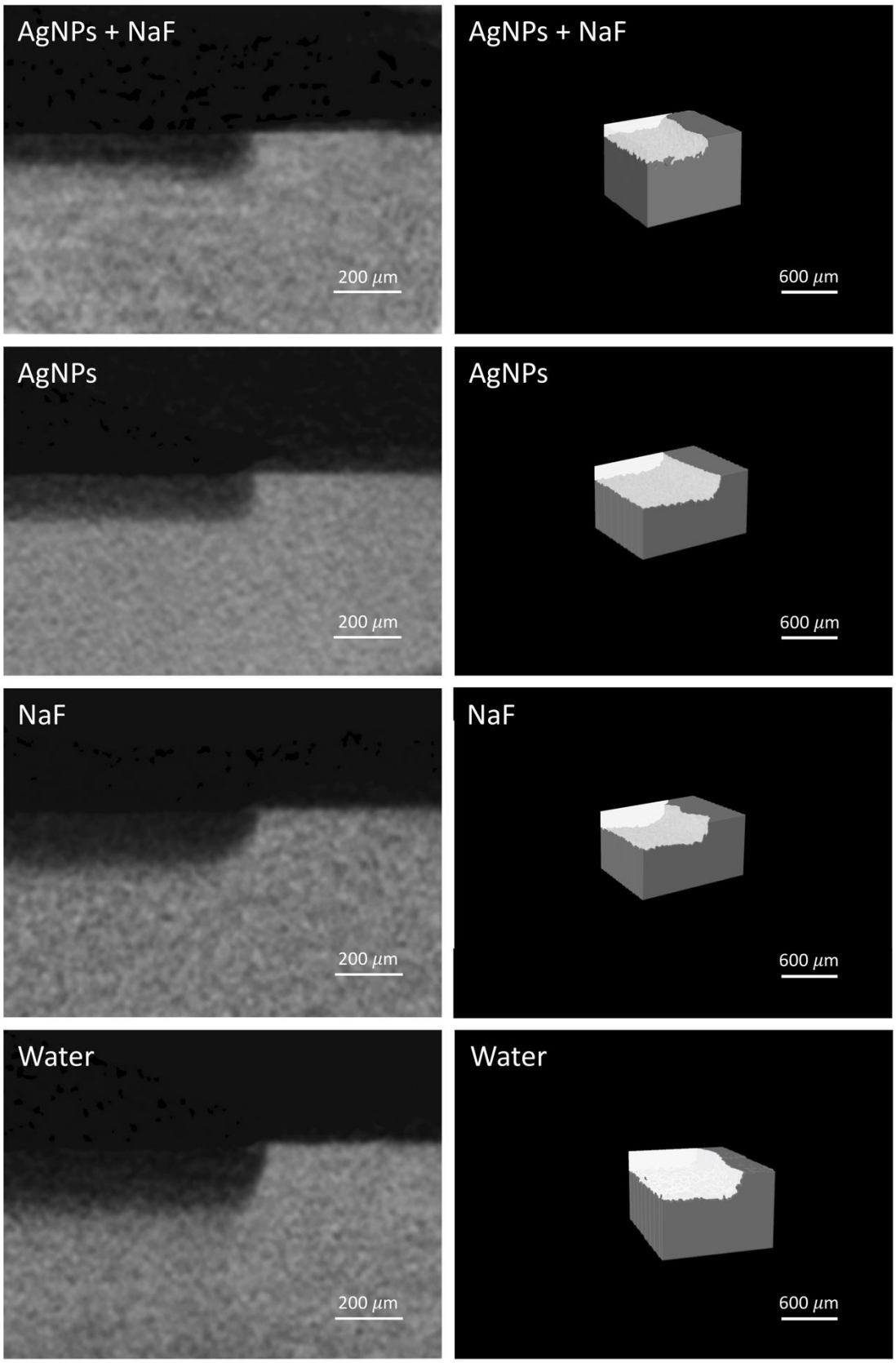

Figure 3. Typical Fourier transform infrared spectra of the four treatment groups' artificial dentine caries.

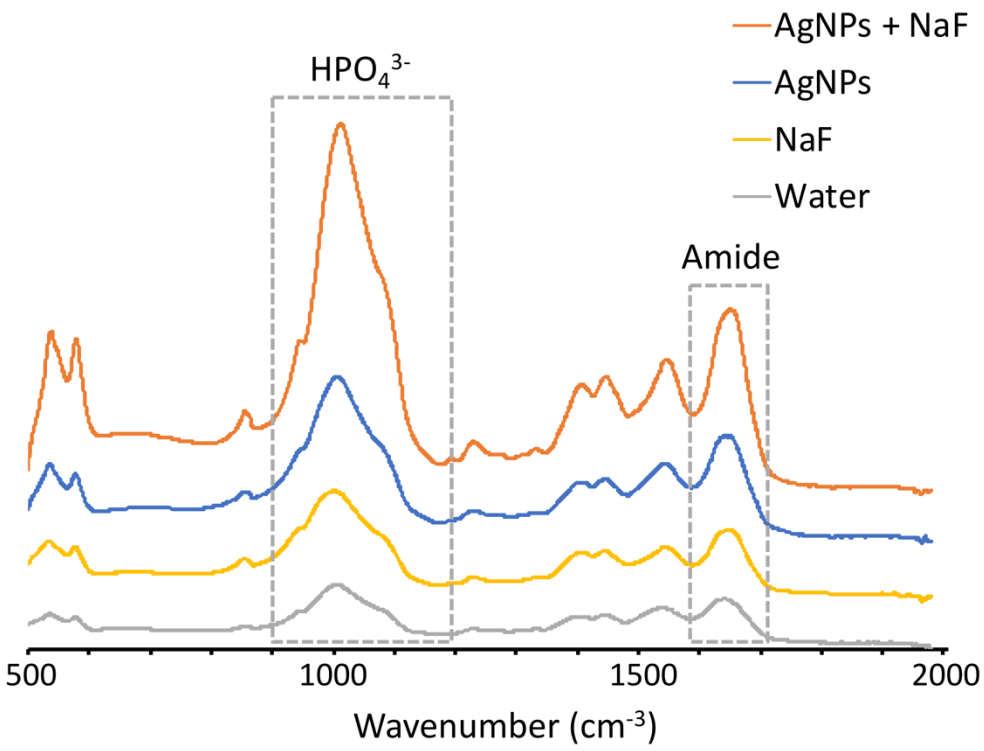

Figure 4. SEM images of the dentine surface morphology in treatment groups.

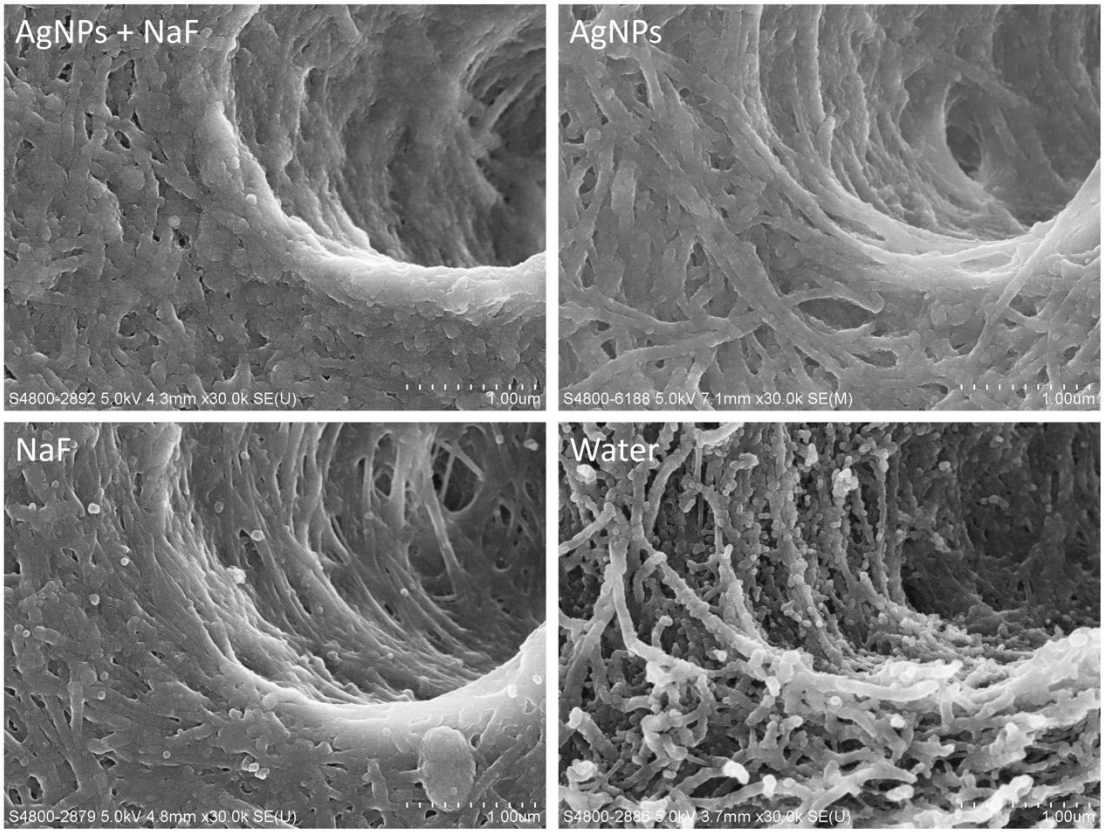

Figure 5. Typical X-ray diffraction patterns of the dentine in four treatment groups.

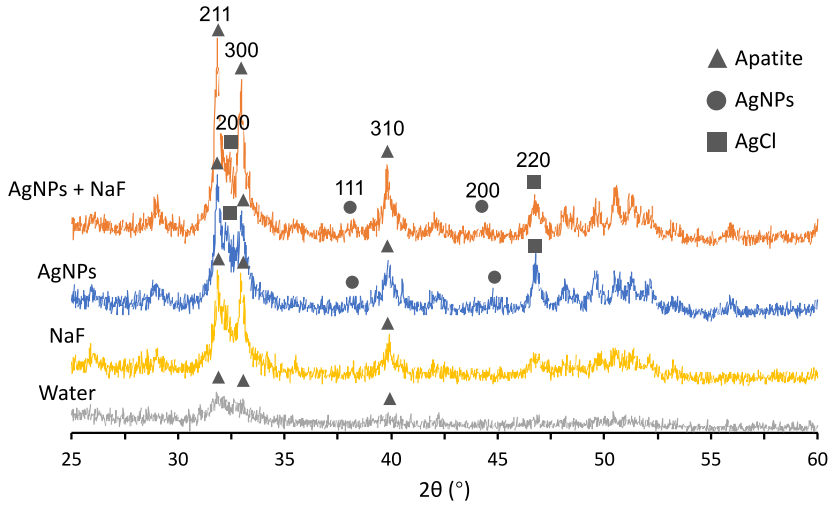

Table 1. Mean values ± standard deviation of lesion depth, surface density and mineral loss of artificial dentine caries in four treatment groups.

Outcome Measurement	Group 1 AgNPs + NaF	Group 2 AgNPs	Group 3 NaF	Group 4 Water
Lesion depth (μm)	151.13 ± 29.13	172.38 ± 23.44	190.41 ± 32.81	221.24 ± 27.91
Mineral loss (g/cm^3)	0.65 ± 0.05	0.77 ± 0.08	0.78 ± 0.07	0.89 ± 0.06

Table 2. Two-way ANOVA of lesion depth, surface density and mineral loss of artificial dentine caries in four treatment groups.

Independent Variable	Lesion depth (μm)	*p* value	Mineral loss (g/cm^3)	*p* value
AgNPs				
Yes	163.59 ± 27.79	< 0.001	0.72 ± 0.09	< 0.001
No	208.76 ± 33.33		0.83 ± 0.08	
NaF				
Yes	167.41 ± 36.09	< 0.001	0.72 ± 0.09	< 0.001
No	193.08 ± 35.04		0.83 ± 0.09	
**p* value	0.40		0.88	

**p* > 0.05 means no significant interaction effect between AgNPs and F.

Table 3. Two-way ANOVA of the ratio of HPO_4^{2-}:amide I in four treatment groups.

Independent Variable		Mean ± SD	*p* value	**p* value
AgNPs				
	Yes	4.92 ± 1.20		
			< 0.001	
	No	3.26 ± 0.93		
				0.13
NaF				
	Yes	4.99 ± 1.15		
			< 0.001	
	No	3.20 ± 0.83		

**p* > 0.05 means no significant interaction effect between AgNPs and F.

Table 4. Mean (±SD) values of L* a* b* coordinates in four groups.

Group	Coordinates	Before	After	*p* value
AgNPs + NaF	L*	59.50 ± 2.40	58.22 ± 3.85	0.17
	a*	19.66 ± 5.01	12.66 ± 0.91	0.006
	b*	33.26 ± 2.87	29.97 ± 3.57	0.16
AgNPs	L*	53.29 ± 3.79	52.67 ± 3.65	0.08
	a*	20.37 ± 2.88	15.56 ± 1.85	< 0.001
	b*	31.28 ± 2.29	28.43 ± 4.45	0.10
NaF	L*	57.50 ± 3.62	56.84 ± 4.46	0.26
	a*	22.57 ± 5.96	15.92 ± 2.57	0.003
	b*	31.71 ± 3.17	28.50 ± 3.25	0.08
Water	L*	54.22 ± 4.20	52.59 ± 3.42	0.13
	a*	19.93 ± 3.38	14.09 ± 0.79	0.003
	b*	30.97 ± 1.78	29.46 ± 5.15	0.37